Magnesium Technology 2012
Edited by: Suveen N. Mathaudhu, Wim H. Sillekens, Neale R. Neelameggham, and Norbert Hort
TMS (The Minerals, Metals & Materials Society), 2012

TENSILE AND CREEP DEFORMATION MECHANISMS IN ROLLED AZ31

Z. Chen[1], C. Boehlert[1,2,3], I. Gutiérrez-Urrutia[4], J. Llorca[2,3] and M.T. Pérez-Prado[3]

[1]Michigan State University, East Lansing, Michigan 48824-1226, USA
[2]Department of Materials Science, Polytechnic University of Madrid, 28040 Madrid, Spain
[3]IMDEA Materials Institute, Calle Profesor Aranguren, s/n, 28040 Madrid, Spain
[4]Max Planck Institute for Iron Research, Max Planck Strasse, 1, 40237 Düsseldorf, Germany

Keywords: Microstructure, Tensile, Slip, Twinning, Creep, Magnesium, Lightweight Alloys

Abstract

Tensile experiments were performed on a rolled AZ31 alloy in an SEM at 323K (50°C), 423K (150°C), and 523K (250°C) in order to analyze the deformation mechanisms *in-situ*. Electron backscatter diffraction (EBSD) was performed both before and after deformation. The mechanical anisotropy was considerably reduced with temperature. Extension twinning was observed at 323K (50°C), but disappeared at 423K (150°C), indicating that the CRSS of non-basal systems becomes smaller than that of twinning at T<423K (150°C). From 423K (150°C) to 523K (250°C), a transition occurred in the dominant deformation mode from basal + prismatic <a> to mainly prismatic <a> slip. This is consistent with a decrease of the CRSS of non-basal slip systems with increasing temperature. *In-situ* tensile-creep experiments, performed at approximately the yield stress at 423K (150°C), indicated less slip and more grain boundary cracking occurs under creep deformation as compared to the higher-stress tensile experiments.

Introduction

The development of lightweight Mg alloys with higher strength requires a detailed knowledge of the deformation mechanisms. Extensive studies have been performed at low strain rates, using conventional *ex-situ* techniques [1-3]. Although widespread values of the critical resolved shear stresses (CRSS) have been reported for the various slip and twinning systems of Mg alloys [4,5], it is generally accepted that the CRSS follows the trend $CRSS_{basal}<CRSS_{\{10\text{-}12\}twinning}<CRSS_{prismatic}<CRSS_{pyramidal}$ at room temperature (RT). The CRSS for basal slip and {10-12} extension twinning are believed to be temperature independent [3]. The CRSS of prismatic and pyramidal systems decrease as the temperature increases, reaching values lower than that of {10-12} extension twinning and, eventually, basal slip [3,6]. Thus, the activity of non-basal slip systems increases with temperature, facilitating intergranular compatibility [1,2,7]. However, this transition temperature is still unclear.

Moreover, the role of grain boundary sliding (GBS) during deformation of Mg alloys at moderate-to-high temperatures is also controversial. Some studies suggested an increasing contribution of GBS at high temperatures, even in materials with conventional grain size [7-9], some also suggested that GBS contributes to deformation even at RT in fine grained Mg alloys [10]. However, these ideas were refuted by some other studies [11].

Highly-textured, rolled AZ31 sheet material shows a significant drop in plastic anisotropy (commonly characterized by the r-value) between 298K (25°C) and 473K (200°C). This behavior was explained in two possible ways. One proposed it to be the result of an increased activity of pyramidal <c+a> slip [2], while the other attributed it to the activation of GBS [7, 12]. Both explanations were supported by their simulation results based on viscoplastic self-consistent modeling.

In this study, *in-situ* deformation characterization was performed during tensile and creep experiments on a rolled AZ31 alloy. Electron backscattered diffraction (EBSD) was performed both before and after the tensile tests. The onset of the different slip and twinning systems as a function of temperature was identified. Further evidence regarding the influence of GBS on the anisotropy was also provided.

Experimental

Rolled and annealed AZ31 sheet of 3mm thickness, was purchased from Magnesium Elektron (Manchester, UK). The sheet material had a strong basal texture. The bulk chemical composition of the as-rolled material, measured using an Inductively Coupled Plasma Analyzer, was Mg-2.9Al-0.73Zn-0.2Mn(wt.%).

Flat dog-bone tensile specimens with gage dimensions of 3 x 2.5 x 10 mm were electro-discharge machined out of the as-received sheet. The samples were machined with the tensile axis either parallel to (RD) or perpendicular to (TD) the rolling direction of the sheets. *In-situ* tensile tests were performed at a constant displacement rate of 0.004mm/s, equivalent to a strain rate of approximately $10^{-3}s^{-1}$, using a screw-driven tensile stage placed inside a Zeiss (Jena, Germany) EVO MA15 SEM at 323K (50°C), 423K (150°C) and 523K (250°C). The temperature was maintained within 5K of the target using a constant-voltage power supply to a 6mm diameter tungsten-based heater located just below the gage section of the sample. Secondary electron (SE) SEM images were taken before loading and during interruptions at various strains throughout the tensile test. The strain values were estimated from the crosshead displacement of the testing machine taking into account the gage length of the samples. Further details of this apparatus and testing technique can be found elsewhere [13]. After the experiments were terminated (usually after achieving 25% strain) and the samples were unloaded, the width and thickness of the samples were measured and compared to those measured before the experiment. These measurements, performed only on the samples tested in the RD, were used to determine the plastic anisotropy. They were compared to previous results on tensile specimens deformed to approximately 10% strain [2,11,12].

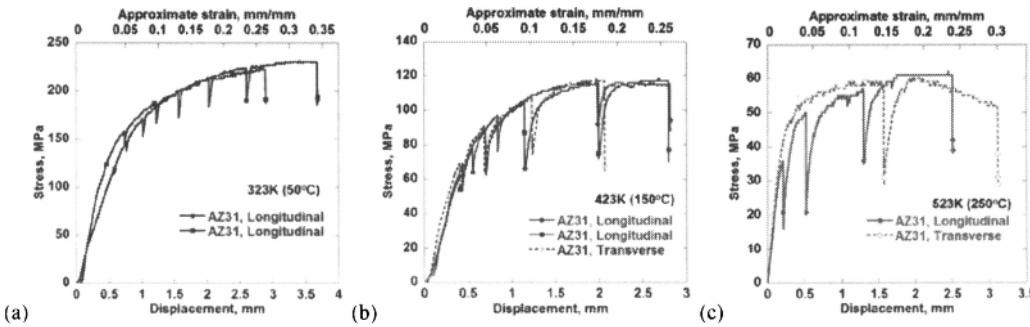

Figure 1. Stress versus displacement plots for samples tensile tested at (a) 323K (50°C), (b) 423K (150°C), and (c) 523K (250°C). The load drops indicate the stress relaxation that occurred when experiment was paused and SEM images were acquired.

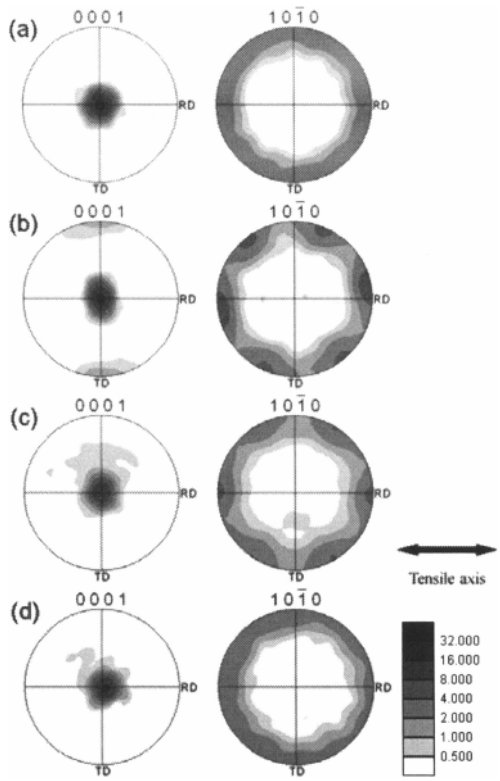

Figure 2. EBSD pole figures along the normal direction (ND) for the AZ31 tensile specimens, (a) un-deformed, the tensile axis is along the RD, (b) tested at 323K (50°C) along RD after ~32.1% strain, (c) tested at 423K (150°C) along RD after ~25.6% strain, and (d) tested at 523K (250°C) along RD after ~24.2% strain. The intensity of the peaks is indicated in the scalebar provided.

The microstructure in a selected area of the specimens (in the center of the gage section) was analyzed before and after each tensile test by EBSD in a 6500 F JEOL field emission gun-scanning electron microscope (SEM) equipped with an EDAX-TSL EBSD system. Sample preparation for EBSD included grinding with 4000 grit SiC paper, mechanical polishing with a 0.5μm silica suspension and final electrochemical polishing for 60s at 20V using the AC2™ commercial electrolyte. The grain size, calculated in the EBSD orientation maps using only grain boundaries with misorientations greater than 15°, was about 13μm. Following a previously described methodology [14], the active slip and twinning systems were identified using the EBSD data and the SEM images acquired during the tensile experiments. Three slip modes and two twinning modes were considered in the deformation analysis: (1) {0001}<-2110> basal <a> slip, (2) {01-10}<2-1-10> prismatic <a> slip, (3) {11-22}<-1-123> second order pyramidal <c+a> slip, (4) {10-12}<-1011> extension twin, and (5) {10-11}<10-1-2> contraction twin.

Two samples, one along RD and one along TD, were creep tested at 423K (150°C) and 75MPa using the same stage described above. SE images were acquired during deformation without interrupting the experiment. EBSD orientation maps were not acquired for the creep-tested specimens, which were not taken to failure but were unloaded after approximately 50 hours of creep.

Results

Tension

The tensile curves for seven specimens tested at different temperatures are shown in Figure 1. Little difference was observed between the RD and TD tests (see Figures 1b and c). The yield strength (YS) was approximately 110MPa at 323K (50°C), 60MPa at 423K (150°C), and 40MPa at 523K (250°C). These values are comparable to those found in the literature for textured AZ31 [15].

Figure 2 shows the EBSD pole figures along the normal direction (ND), for specimens before testing, and after testing at 323K (50°C), 423K (150°C), and 523K (250°C). The as-rolled AZ31 sheet exhibited a basal fiber texture in which the basal plane was parallel to the rolling plane, typical of rolled and annealed Mg alloys [16]. The basal texture was maintained after deformation at 323K (50°C). The alignment of (10-10) poles with the RD (tensile axis) revealed the occurrence of prismatic slip. A new texture component, (0001) parallel to the TD direction, was developed, which revealed the activation of extension twinning. At 423K (150°C), samples tested along RD and TD developed a similar deformation texture, and it was similar to that observed at 323K (50°C). However, the texture component <0001>//TD was not observed in the sample deformed at 423K (150°C), which indicated that twinning was not active at 423K (150°C). At 523K

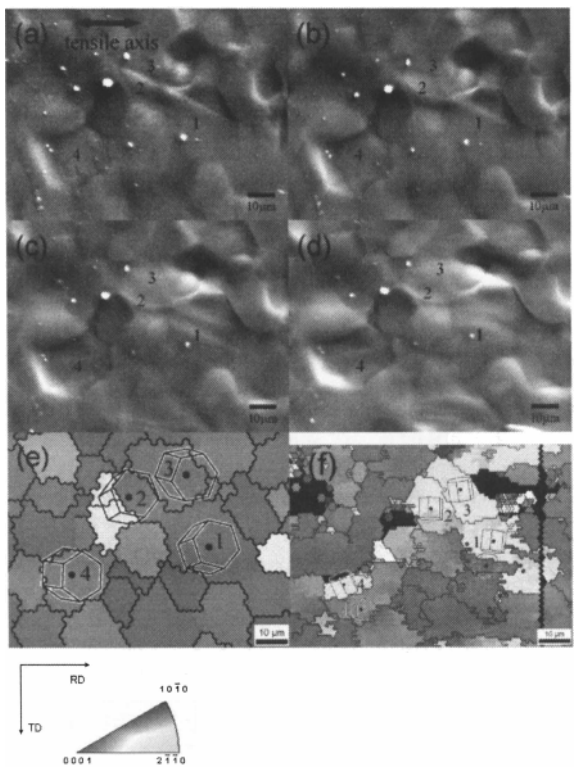

Figure 3. SE SEM images for a sample tested at 323K (50°C) along RD corresponding to approximate strain of: (a) 5.4% strain, (b) 10.9% strain, (c) 21.2% strain, and (d) 32.1% strain, (e) EBSD IPF map in the ND before test, and (f) EBSD IPF map in the ND after test. Twinning was observed in the grains labeled 1-4 after strains of greater than 5.4%.

Table I. Twinning modes observed in Figure 3

Grain	Orientation relationship between reoriented region and parent grain	Twin type	Schmid Factor
1	89.7°@<11-20>	(-1102)[1-101]	0.05
2	88.0°@<11-20>	(-1102)[1-101]	0.05
3	89.7°@<-12-10>	(-1012)[10-11]	0.08
4	89.6°@<-2110>	(0-112)[01-11]	0.05

(250°C), samples tested along RD and TD also developed a different texture than that formed at lower temperatures (323-423K (50-150°C)). Basically, no texture variation with respect to the initial texture was developed at 523K (250°C), indicating that plastic strain was controlled by different dominant deformation modes than those controlling plasticity at lower temperatures.

At 323K (50°C), twinning was observed during the early stages of deformation (147-171MPa/~2.9-5.4% strain). Slip traces were observed after the sample reached approximately 5% strain, but not in large quantities. Furthermore, some cracks became apparent at the grain boundaries as the deformation increased. Figure 3 shows SEM images of the same region taken at different stages of the tensile test. Deformation twins were found in grains referred as to 1, 2, and 3 at ~5.4% strain, and in grain 4 at ~21.2%

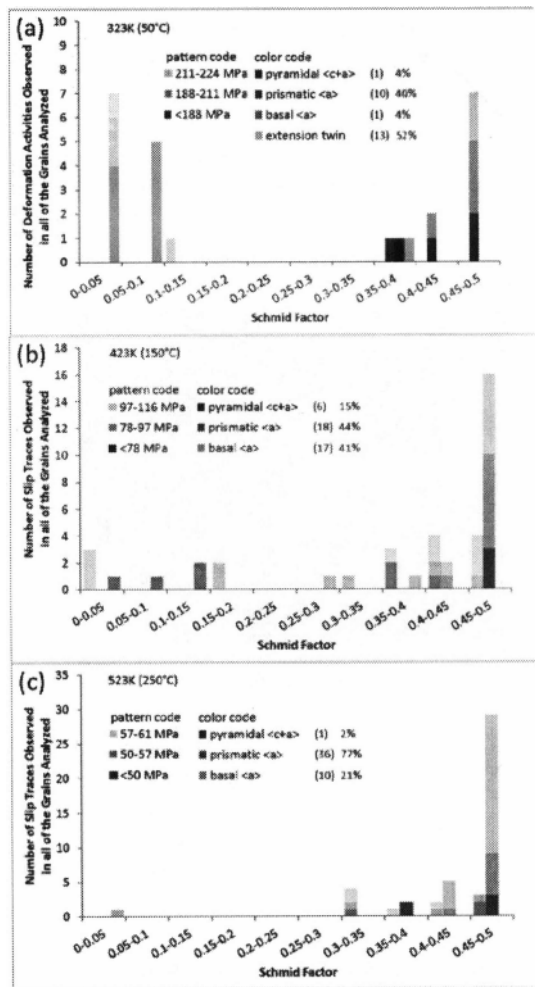

Figure 4. Schmid factor distributions and stress levels at which the activities of each of the deformation modes were observed for samples tensile tested at (a) 323K (50°C), (b) 423K (150°C), and (c) 523K (250°C).

strain. As the deformation proceeded, the twin area fraction increased, and ultimately consumed a large part of the parent grain. The lattice orientations of the grains with twinning are indicated by the unit cells drawn on the inverse pole figure (IPF) map for this region both before and after the tensile test (Figure 3e and 3f). The orientation relationships between the reoriented region and the parent grain, see Table I, suggests the formation of {-1102}<1-101> extension twin. This deformation mode, which ideally reorients the lattice 86.5° about the <11-20> direction and leads to extension along the c-axis, was not favorable in most of the grains considering the basal texture in the material. However, extension twinning under tension along RD in AZ31 sheet has been observed occasionally [15]. The Schmid factors for twinning were small, suggesting that twinning is easily activated at RT compared to the other deformation modes. In the two samples tested at 323K (50°C), 13 grains were observed to reorient due to extension twinning, and no contraction twins were observed. Slip was observed in 12 grains. Figure 4(a)

summarizes the Schmid factor distribution and stress levels at which the identified deformation modes were observed. Among the 12 slip traces analyzed, 1 was basal <a> slip, 10 were prismatic <a> slip, and 1 was pyramidal <c+a> slip.

At 423K (150°C), no twinning was observed during the *in-situ* test. Slip bands were first observed between approximately 4.0-8.5% strain, and an increase in the density of slip bands can be clearly observed with increasing strain. The appearance of some grain boundary ledges could be distinguished after approximately 1.1% strain. As the deformation proceeded, some grain boundary cracks became apparent. Figure 5 illustrates a region in a sample

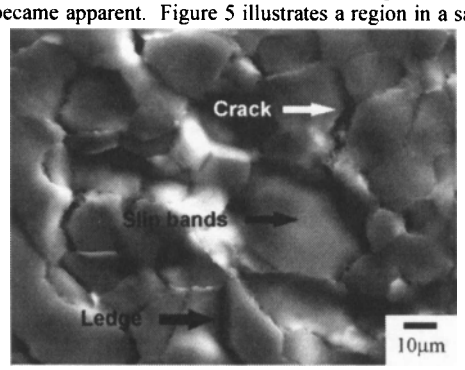

Figure 5. SEM images for a sample tested at 423K (150°C) along RD; at approximately 25% strain.

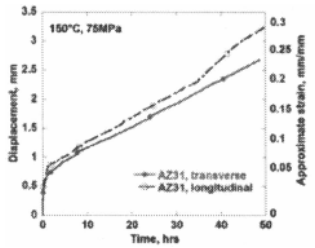

Figure 6. Creep displacement versus time plot for rolled AZ31 at T=423K (150°C) and σ=75MPa.

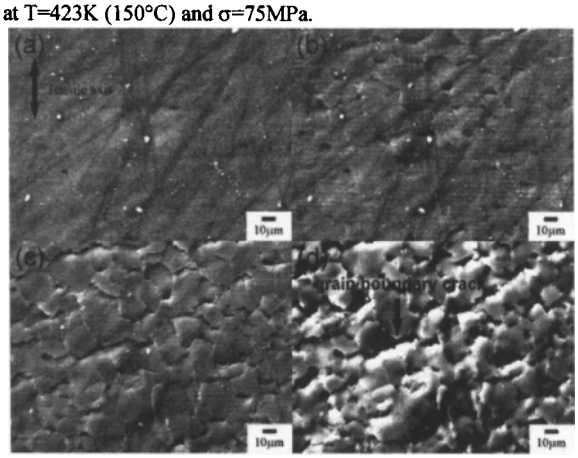

Figure 7. SE SEM images taken for the same area of a sample creep test at T=423K (150°C) along TD. The creep time and approximate strain are (a) 0.1 hrs, 1.4%, (b) 0.4 hrs, 2.9%, (c) 12.0 hrs, 9.4%, and (d) 45.6 hrs, 22.9%. Grain boundary cracking was prevalent.

tested along RD, where slip bands, grain boundary ledges and cracks were indicated. In the three samples tested at 423K (150°C), the active slip systems were determined for 41 different slip trace, among which 17 were basal <a> slip, 18 were prismatic <a> slip, and 6 were pyramidal <c+a> slip, see Figure 4(b). Basal slip and pyramidal <c+a> slip occurred over a wide range of Schmid factors and stresses, while prismatic <a> slip was activated only when a high Schmid factor (>0.4) was present.

In the samples tested at 523K (250°C), the slip traces were more obvious than in the samples tested at 323K (50°C) and 423K (150°C). As the deformation proceeded, some grain boundary relief was also observed. The slip systems were determined for 47 slip traces in the two samples tested at 523K (250°C): 10 were basal <a> slip, 36 were prismatic <a> slip, and 1 was pyramidal <c+a> slip, see Figure 4(c). Most of the active slip systems exhibited a relatively high Schmid factor (>0.30). Thus, it appeared that prismatic <a> slip became dominant and more easily activated at higher temperatures compared to basal slip.

Creep

Creep strain versus time curves are shown in Figure 6 for samples tested along RD and TD at σ=75MPa and T=423K (150°C). The common primary and secondary stages of creep were exhibited. There was little difference between the different orientations in terms of the creep strains and strain rates. Grain boundaries served as crack nucleation sites in creep, see Figure 7. No slip traces were observed. It is noted that during the 423K (150°C) tensile test, 3 basal slip traces and 3 prismatic <a> slip traces were observed at stress less than 78MPa, the latter only for Schmid factors between 0.4 and 0.5.

Discussion

Twinning and Dislocation Slip

The EBSD pole figures shown in Figure 2 were consistent with previous studies [2] and revealed that, when the AZ31 sheet alloy was deformed along an in-plane direction at 323K (50°C) and 423K (150°C), prismatic slip was prevalent. This lead to the alignment of the (10-10) poles parallel to the tensile axis. Basal slip should also be favorable in grains which deviated from the perfect basal orientation. However, when deformation took place at higher temperature (523K (250°C)), the initial basal fiber remained, yet the (10-10) poles were not aligned parallel to the tensile axis according to the pole figures (see Figure 2(d)). Thus, the dominant deformation modes at this temperature could not be easily inferred from examination of the pole figures.

The variation with temperature of the CRSS of various slip and twinning systems in Mg alloys has been studied by both crystal plasticity models in polycrystals and experiments in single crystals. The CRSS of basal slip and extension twinning are generally believed to be temperature independent [3]. Using the output of a full constraint Taylor model proposed by Barnett [3], the CRSS of prismatic and pyramidal slip are predicted to become smaller than that of extension twinning at temperatures higher than 506K (233°C) and 473K (200°C), respectively, and they remain higher than that of basal slip until about 733K (460°C). Based on single crystal experiments, Chapuis and Driver [6] reported that the CRSS of pyramidal slip was higher than that of

prismatic slip within the temperature range investigated and that neither of them became comparable to that of extension twinning until temperatures as high as 723K (450°C). Earlier studies on the subject [17], carried out also in single crystals in a temperature range from 298-773K (25-500°C), confirmed that the CRSS for pyramidal <c+a> slip is higher than that of prismatic <a> slip, although the latter becomes comparable to that of extension twinning at temperatures higher than 473K (200°C). Thus, large discrepancies still remain between various studies regarding the critical temperatures at which the CRSS of non-basal systems become comparable to that of extension twinning and basal slip. Furthermore, the relative activity of the different deformation mechanisms in the temperatures ranges of interest is not well understood.

Our *in-situ* experiments provided new insight on these issues. The relative contributions of the different slip systems at 423K (150°C) were the following: 41% basal, 44% prismatic <a>, and 15% pyramidal <c+a>. The relative contributions of the different slip systems at 523K (250°C) were: 21% basal, 77% prismatic <a>, and 2% pyramidal <c+a>. The present work showed that from 423K (150°C) to 523K (250°C), a transition in the dominant deformation mechanism occurred from basal + prismatic <a> to mainly prismatic <a> slip. Basal slip took place at 423K (150°C) even in grains in which the Schmid factor is very low (as low as 0.05) (see Figure 4(b)). Conversely, 16 out of the 18 prismatic slip traces occurred in grains in which the corresponding Schmid factor was greater than 0.45. This suggests that the CRSS for prismatic slip is still significantly higher than that of basal slip at 423K (150°C). However, it must be already lower than that of twinning, as twinning was absent at 423K (150°C). The increase in the contribution of prismatic slip with temperature, from 44% at 423K (150°C) to 77% at 523K (250°C), suggests that the CRSS for prismatic slip might be on the order of that of basal slip at 523K (250°C). The present observations provided by the *in-situ* tests on polycrystals seem to be more in agreement with earlier experimental single crystal studies [17] than with the other works, and close to the transition temperature predicted by crystal plasticity models [3]. These comparisons must be, however, taken with caution, as the CRSS values provided by single crystal experiments do not directly reflect the applied shear stress that is necessary to activate certain deformation systems in polycrystalline materials since most hardening contributions are not proportional to the CRSSs but are additive to them [4]. It is noteworthy that the activity of pyramidal <c+a> slip, which was 4% at 323K (50°C), 15% at 423K (150°C) and 2% at 523K (250°C), remained low in the temperature range analyzed in the current study.

Grain Boundary Sliding

The role of GBS during deformation of Mg alloys is controversial [2,7-11]. In the current *in-situ* observations, no significant differences were revealed between the amount of grain boundary cracking and of jogging of fiducial lines, both potential signs of GBS, between the three different temperatures for tensile test. In turn, as described above, a clear variation between the relative activities of the various slip systems was detected. However, during the creep test at 423K (150°C) and 75MPa, a significant decrease of the slip activity accompanied by an increase of the incidence of grain boundary cracking and jogging of fiducial cracks, was clearly observed. These observations suggest that GBS does indeed contribute to the total strain under these conditions. However, the contribution of GBS to the total applied strain was small even at temperatures as high as 250°C at constant strain rates of $10^{-3}s^{-1}$ for the tensile experiments. This is consistent with the fact that the creep test took place at much lower strain rates (the strain rate corresponding to the secondary stage was approximately $1.1x10^{-6}$ s^{-1}), at which it might have been assisted by diffusion, which would take place much more easily.

Origin of the Decrease in Anisotropy at Higher Temperatures

Figure 8 compares the r-values of rolled AZ31 as a function of temperature, including the results of the current study. Our results showed that there was a considerable drop in the r-value with temperature, and this is in agreement with previous data [2,11,12]. The decrease in anisotropy with increasing temperature has been attributed to an increase of the contribution of GBS [7,12] or to the enhanced operation of pyramidal <c+a> slip [2,11] with increasing temperature. Stanford *et al.* [11] showed that increasing the relative activity of pyramidal <c+a> slip by only 15%, with a commensurate decrease in prismatic slip activity, led to a reduction of the normal anisotropy by a factor of two. Their observations suggested that the reduction in the r-value was likely caused by an increase in non-basal slip activity as they did not observe any significant contribution of GBS. In the current work, the proportion of non-basal slip activity (primarily prismatic <a>) significantly increased with temperature, and there was no significant difference between GBS at each of the temperatures examined. Although our data do not reveal an increase in the activity of pyramidal <c+a> slip, as reported in [2], the present results suggest that the observed decrease in anisotropy might be due to increased non-basal activity, rather than to GBS.

Creep

As expected, little difference were observed between samples tested in the RD and TD. Grain boundaries served as crack nucleation sites in creep, see Figure 7, and grain boundary cracking may have been accommodating GBS. There are two well described accommodation mechanisms for GBS: diffusion [18] and slip [19]. GBS accommodated by diffusion is typically observed at high temperature, such as those encountered during creep. In this model, the cavity created by the relative movement of one grain past another is filled by diffusing atoms. This mechanism allows for a shape change of the grains during the deformation. The other accommodation mechanism for GBS is slip. When two grains slide past each other, stresses accumulate at the grain boundary, which are released by the intragranular movement of dislocations. Of the two accommodation

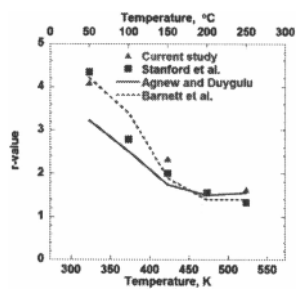

Figure 8. The r-value measured after a tensile strain for the current study as compared with previous studies [2,11,12].

mechanisms, the former is more likely for the conditions evaluated in the present work as grain boundary cracking, rather than slip, was observed [20].

Conclusions

Rolled AZ31 was *in-situ* tensile tested in an SEM at temperatures of 323K (50°C), 423K (150°C), and 523K (250°C), and EBSD orientation maps were acquired both before and after the deformation on the same local microstructural patch. Twinning was observed at 323K (50°C), but disappeared at 423K (150°C). The deformation at high temperature was controlled by a combination of basal and prismatic <a> slip. From 423K (150°C) to 523K (250°C), a transition in the dominant deformation mechanism occurs from basal + prismatic <a> to mainly prismatic <a> slip. A significant drop in the normal anisotropy was exhibited with increasing test temperature. Observation of grain boundary offsets and grain boundary cracking during the tensile deformation confirmed that GBS was present. However, it did not significantly contribute to the overall total strains and appeared to be insensitive to temperature. Therefore the reduction in normal anisotropy with temperature was more likely due to the increased slip activity of the non-basal slip systems rather than to GBS.

In addition, two *in-situ* creep tests were performed at σ=75MPa and T=423K (150°C). Slip traces were not observed, while cracking preferentially occurred at grain boundaries and fiducial markings indicated jogs at grain boundary locations. Thus creep deformation was dominated more by GBS than slip activity, and therefore grain boundaries play a more important role during creep than during tension.

Acknowledgments

This work was supported by the National Science Foundation Division of Material Research (Grant No. DMR1107117). CJB acknowledges the support from the Spanish Ministry of Education for his sabbatical period in Madrid (SAB2009-0045). The authors would like to thank the vehicle interior manufacturer, Grupo Antolin Ingeniería, S.A., within the framework of the project MAGNO2008-1028-CENIT funded by the Spanish Ministry of Science and Innovation.

References

1. A. Couret and D. Caillard, "An Insitu Study of Prismatic Glide in Magnesium .2. Microscopic Activation Parameters", *Acta Metallurgica*, 33 (8) (1985), 1455-1462.

2. S.R. Agnew and O. Duygulu, "Plastic Anisotropy and the Role of Non-basal Slip in Magnesium Alloy AZ31B", *Int J Plast*, 21 (6) (2005), 1161-1193.

3. M.R. Barnett, "A Taylor Model Based Description of the Proof Stress of Magnesium AZ31 during Hot Working", *Metall Mater Trans A*, 34A (9) (2003), 1799-1806.

4. W.B. Hutchinson and M.R. Barnett, "Effective Values of Critical Resolved Shear Stress for Slip in Polycrystalline Magnesium and Other HCP Metals", *Scr Mater*, 63 (7) (2010), 737-740.

5. M.R. Barnett *et al.*, "A Semianalytical Sachs Model for the Flow Stress of a Magnesium Alloy", *Metall Mater Trans A*, 37A (7) (2006), 2283-2293.

6. A. Chapuis and J.H. Driver, "Temperature Dependency of Slip and Twinning in Plane Strain Compressed Magnesium Single Crystals", *Acta Mater*, 59 (5) (2011), 1986-1994.

7. B. Hutchinson *et al.*, "Deformation Modes and Anisotropy in Magnesium Alloy AZ31", *Int J Mater Res*, 100 (4) (2009), 556-563.

8. J.A. Del Valle *et al.*, "Deformation Mechanisms Responsible for the High Ductility in a Mg AZ31 Alloy Analyzed by Electron Backscattered Diffraction", *Metall Mater Trans A*, 36A (6) (2005), 1427-1438.

9. J.A. Del Valle and O.A. Ruano, "Separate Contributions of Texture and Grain Size on the Creep Mechanisms in a Fine-Grained Magnesium Alloy", *Acta Mater*, 55 (2) (2007), 455-466.

10. J. Koike *et al.*, "Grain-Boundary Sliding in AZ31 Magnesium Alloys at Room Temperature to 523 K", *Mater Trans*, 44 (4) (2003), 445-451.

11. N. Stanford *et al.*, "Deformation Mechanisms and Plastic Anisotropy in Magnesium Alloy AZ31", *Acta Mater*, 59 (12) (2011), 4866-4874.

12. M.R. Barnett *et al.*, "Role of Grain Boundary Sliding in the Anisotropy of Magnesium Alloys", *Scr Mater*, 61 (3) (2009), 277-280.

13. C.J. Boehlert *et al.*, "In situ Scanning Electron Microscopy Observations of Tensile Deformation in a Boron-Modified Ti-6Al-4V Alloy", *Scr Mater*, 55 (5) (2006), 465-468.

14. C.J. Boehlert *et al.*, "Slip System Characterization of Inconel 718 Using In-Situ Scanning Electron Microscopy", *Advanced Materials & Processes*, 168 (11) (2010), 41-45.

15. A.S. Khan *et al.*, "Mechanical Response and Texture Evolution of AZ31 Alloy at Large Strains for Different Strain Rates and Temperatures", *Int J Plast*, 27 (5) (2011), 688-706.

16. A.D. Rollet and S.I. Wright, "Typical Textures in Metals", *Texture and Anisotropy*, ed. U.F. Kocks, et al. (Cambridge, Cambridge University Press, 1998), 179-239.

17. T. Obara *et al.*, "[11-22](-1-123) Slip System in Magnesium", *Acta Metallurgica*, 21 (7) (1973), 845-853.

18. M.F. Ashby and R.A. Verrall, "Diffusion-Accommodated Flow and Superplasticity", *Acta Metallurgica*, 21 (2) (1973), 149-163.

19. A.K. Mukherje, "Rate Controlling Mechanism in Superplasticity", *Mater Sci Eng*, 8 (2) (1971), 83-89.

20. C.J. Boehlert *et al.*, "*In-situ* Analysis of the Tensile and Tensile-Creep Deformation Mechanisms in Rolled AZ31", *Acta Mater*, in print.